# *Drosophila grainyhead* gene and its neuroblast-specific enhancers show epigenetic synchrony in the cells of central nervous system.

Rashmi Sipani[1, 2, 5], Yamini Rawal[1, 3, 5], Jiban Barman[1, 2, 5], Prakeerthi Abburi[1], Vishakha Kurlawala[1] and Rohit Joshi[1, 4]

1- Laboratory of Neuroscience and Cell Biology, Centre for DNA Fingerprinting and Diagnostics (CDFD), Inner Ring Road, Uppal, Hyderabad-500039. India.

2- Graduate Studies, Manipal Academy of Higher Education, Manipal 576104.

3- Graduate studies, Regional Centre for Biotechnology, Faridabad 121001.

4- Corresponding author rohit@cdfd.org.in; rj2152@gmail.com

5- Contributed Equally

**Data Availability Statement:** All relevant data are within the manuscript and its Supporting Information files.

**Abstract**

The enhancers are the epicentre of multicellular gene regulation. Therefore, their role in transcription needs to be functionally validated by deleting them, which will then serve as a central point for understanding the epigenetic/molecular basis of tissue-specific gene regulation. We have attempted this by identifying a subset of enhancers regulating the neural progenitor (neuroblast-NB) specific expression of the *Drosophila grainyhead* (*grh*) gene, a transcription factor known for its role in

epithelial cell fate determination and CNS development. To this end, we isolated seven new enhancers of *grh* and generated single and double deletions for two of the NB-specific enhancers. While the single deletions did not have much impact on the Grh expression, the double deletion resulted in a significant reduction in the expression of Grh in CNS, which resulted in NB proliferation defect and a block of abdominal NB apoptosis. The comparative analysis of the epigenetic state of the *grh* and its NB-specific enhancers indicates that the two are broadly in sync with each other across the three cell types of the CNS. Our experiments also suggest that *grh* is mainly transcribed in the NBs and it is Grh protein that GMC inherits. Collectively, we report functional identification of one subset of enhancers regulating *grh* expression in the NBs; our work also underlines the importance of enhancer deletion in establishing their functional role in tissue-specific gene regulation.

## Introduction

The gene transcription in multicellular organisms is highly complex and often relies on multiple enhancers (Cis-Regulatory Elements-**CREs**) to fine-tune spatial and temporal dynamics of the gene expression. The *lacZ* reporter assays have been standard for identifying new CREs. However, besides enhancer deletion, there is no easy way to establish whether a CRE is required for gene expression in a particular tissue. With the advent of CRISPR-Cas9 technology [1-3], it is now possible to precisely delete CREs and address their role in tissue-specific gene regulation and development. Such functional validation will give credibility to the associated biochemical, genetic and epigenetic experiments and provide physiologically relevant insights into gene regulation.

*Drosophila* offers sophisticated genetic tools like CRISPR-Cas9 [4, 5], which enables precise deletion of the enhancer, and Targeted DamID (**TaDa**) [6], which allows probing the chromatin status of the gene/enhancer in a tissue-specific manner. TaDa technique, coupled with next-generation sequencing (referred to as **TaDa-Seq**), has been used successfully to assay the chromatin landscape of the neural stem cells (Neuroblasts- **NB**), intermediate progenitors (Ganglion Mother Cells-**GMCs**) and neurons of the developing Central Nervous System (**CNS**) [7]. However, despite these advances, the in-vivo cell-specific chromatin status of a functionally validated tissue-specific enhancer has not been probed. Similarly, how the epigenetic status of a gene correlates with cell-specific enhancers and how it changes across different cell types of CNS in vivo remains unexplored. In this work, we have attempted this by identifying and deleting a subset of NB-specific enhancers for the *Drosophila grh* gene.

*Drosophila grainyhead* (***grh***) and its vertebrate orthologs (Grainyhead-like, **Grhl-1-3)** code for basic helix-loop-helix transcription factor (**TF**) [8, 9] [10] [11] [12-14] which function as a master regulator of epithelial cell fate and are crucial for maintenance and homeostasis of epithelial cells [12-17]. In *Drosophila* Grh has also been shown to function as a pioneer TF and regulate the chromatin accessibility of its target genes [13, 14, 18-20]. In developing CNS of *Drosophila* Grh expresses in the Type I NBs and their GMCs as early as stage 15 of embryogenesis [8] and contributes to neuronal diversity by functioning as a temporal series transcription factor (**tTFs**) in Type I NBs during embryonic stages [21-24] and in Intermediate Progenitor Cells (**INPs**) of the Type II NBs during the larval stages [22-25]. Grh also plays a segment-specific role in the proliferation of thoracic NBs [13, 26, 27] and Hox-dependent apoptosis of abdominal and terminal NBs [26, 28-32]. However, despite its importance in neural and non-neural tissues, little is known about the mechanisms regulating the expression of Grh (and its vertebrate orthologs) in vivo [33-35]. In *Drosophila*, only two genomic regions have been shown to regulate the *grh* expression in NBs, while none has been identified for epithelial tissue. The two regions are a 4 Kb enhancer (which also covers a 1.3 Kb *grh-NRE* CRE) located in the second intron [12, 36] and a 1.5 kb region in the seventh intron of the gene [37]. Neither of these enhancers has been deleted to functionally test for their role in regulating *grh* expression in NBs of CNS.

Following up on this, we checked 11 genomic regions by *lacZ* reporter assay and identified seven new potential CREs that may regulate Grh expression in larval NBs and wing discs. Thereafter, we used CRISPR-Cas9 to delete and functionally validate the role of two enhancers in regulating the NB-specific expression of the *grh* gene in *Drosophila*. We find that the homozygotes for the single deletions were

viable as adults and did not significantly affect Grh expression in larval NBs. The trans-heterozygotes for the double deletion (*grh*$^{DD}$) and *grh* deficiency (*grh*$^{DD}$/*grh*$^{Df}$) eclosed as adults after a mild developmental delay and the larval CNS showed a significant decrease in the expression of the Grh from the NBs, and a complete loss of Grh from a small minority of NBs, while leaving the expression of Grh in the wing disc unaffected. This also resulted in a proliferation defect and a block of NB apoptosis in the larval ventral nerve cord (**VNC**). Thereafter, we re-analysed published TaDa data for NBs, GMCs and neurons for the five representative chromatin-binding proteins (RNA Pol II-RNAP, Brahma-Brm, HP1a, Pc and H1) [7] to examine the chromatin status of NB-specific enhancers and correlated it with that of the *grh* gene in different cell types of CNS. The comparative analysis suggests that the chromatin state of Grh and its NB-specific enhancers are broadly in sync with each other across the three cell types of the CNS. This analysis indicated that Grh is mainly transcribed in the NBs and not in GMC and neurons, an observation also corroborated by smFISH, suggesting that it is Grh protein that is inherited from NBs to GMCs. Collectively, we report functional identification of one subset of enhancers regulating the *grh* expression in the NBs of the CNS. Our deletion experiments underline the importance of functional validation of CREs to understand their contribution to tissue-specific gene regulation. Considering the role of *grh* as a tTF and a pioneer factor, this work provides the preliminary groundwork for exploring its complex transcriptional regulation both in neural and non-neural tissues.

## Results

### Expression analysis of *grh* enhancers.

To identify the minimal enhancer region within the 4Kb CRE of *grh* (*grh4 or grh-NB,* referred to as *Int-2B* here, Fig 1A and S1A), which expresses strongly in the

NBs of larval CNS [12], we subfragmented this region. A 1.2 Kb sub-fragment of *Int-2B* (*Int-2BF1,* Fig 1B and 1C) was found to recapitulate the expression of the entire 4 Kb region, while the other two fragments (*Int-2BF2* and *Int-2BF3*) did not express in larval CNS. This 1.2 Kb region was further narrowed to 150 bps, which had to be trimerised to show significant activity in larval NBs (Fig S1 and Sup Data). *Int-2BF1* overlapped with a previously reported 1.3 Kb enhancer (*grh-NRE*) [36] (Fig 1A). Since Grh and *grh-NRE* are known to be sensitive to Notch signalling in Type-II NBs of larval CNS [36], we tested if the same happens for *Int-2BF1* in Type-I NBs. We observed that though *Int-2BF1-lacZ* showed partial downregulation in NBs, only a few cells showed Grh downregulation (Fig 1D and 1E'), suggesting that Grh expression in Type-I NBs is largely insensitive to Notch signalling.

Next, we screened 11 non-coding genomic regions bracketed within two modENCODE class I insulator elements identified for *grh* gene [38] (detailed in sup Data) and identified seven new CREs (*Ex1up, Int-2C, Int-8, 9, 10, 11, 14* using reporter-lacZ assay) for their expression in the larval NBs (both Type-I and Type-II) and the wing disc tissue (Fig 1F-1J, Fig S2, Fig S3, expression also summarised in Table I). We observe that, except for *Ex1up*, none of the other CREs were expressed in the wing disc (Fig S3).

In contrast to most NBs in the brain and VNC, the NBs in the A8-A10 segment do not express Grh in early larval stages and show a gradual increase in Grh expression and Notch activity from mid-larval stages, resulting in their apoptosis [31]. Using this increase in Grh expression as a proxy for temporal dynamics of Grh, we found that five out of a total of nine CREs could successfully recapitulate Grh expression and dynamics in A8-A10 NBs before they died in the mid-L3 stage (Table

I). This included three of the new CREs (*Ex1up, Int-2C,* and *Int-14*) (Fig S4D-S4I and Table I) and two already known CREs (*Int-2BF1* and *Int-7*, Fig S4A-S4C, Table I).

Based on the uniformity, temporal dynamics and strength of their expression in larval NBs, the enhancers (both novel and known [in bold]) were divided into three categories. The first category included the ones which showed strong and uniform expression in the majority of the NBs (*Ex1up,* ***Int-2BF1****, Int-2C, Int-14*) (Fig 1C, 1F-1J, Fig S2E and S2J). The second category CREs were very weak in their expression in NBs (*Int-8, Int-9* and *Int-11*) (Fig S2B-S2D and S2G-S2I). The third category included the remaining two enhancers (***Int-7***, *Int-10*), of which *Int-7* showed strong but variable expression in the NBs, and *Int-10* showed strong expression in Type II NBs and very limited and weak expression in Type I NBs (detailed in Sup Data and Fig S2A and S2F, and S2K-S2L), suggestive of *Int-10* being a central CRE for the regulation of *grh* in Type II NBs. We also compared the expression of our *enhancer-lacZ* lines with the FlyLight project and found that our expression largely matched those of FlyLight lines (Sup Data).

Collectively, we report identifying seven new CREs for the *grh* gene (*Ex1up, Int-2C, Int-8, 9, 10, 11, 14*), which, along with the existing two enhancers (*Int-2BF1* and *Int-7*), may play a role in regulating the expression of Grh in neural and non-neural tissues.

**Grh expression in NBs is unaffected in individual deletion for *Int-2BF1* and *Int-2C***

Next, we focused on three of the four CREs from the first category (*Ex1up-2.7kb,* ***Int-2BF1-1.1kb*** and *Int-2C-1.5kb*) owing to their relative proximity with each other (Fig 2G) and considering that they presented an opportunity to functionally

check whether their deletion would affect the *grh* expression exclusively in NBs, wing discs, or both. We used the double guide CRISPR-Cas9 approach to delete these CREs [4]. We could successfully generate stable single deletions for *Int-2BF1* and *Int-2C* (*ΔInt-2BF1* and *ΔInt-2C*) (Fig 2A and 2B and Table II). However, both these single deletions were homozygous viable and fertile as adults, homozygotes for these deletions did not show any significant change in Grh expression in NBs (Fig 2C-2F and C''' and E''').

The Grh have neural (GrhO and O') and non-neural (GrhN and N') isoforms (Fig 1A'). The CNS-specific O-isoforms have two additional exons (exon-4 and 5), which code for 205 residues [13]. The polyclonal Grh antibody used by us is expected to identify both kinds of isoforms. Since *Int-2BF1* and *Int-2C* deletions showed no decrease in the levels of the Grh in NBs, we considered the possibility that both the isoforms might be expressed in NBs and deletion of a given CRE altered the expression of the GrhO isoform without affecting GrhN isoform in NBs. To test this, we generated a GrhO-specific polyclonal antibody against 205 residues of exon-4 and 5. We found that the Grh Exon 4+5 antibody stained exclusively NBs and GMCs in CNS (inset Fig-S5A') but not the cells in the eye (Fig S5C' vs S5B') and wing imaginal discs (Fig S5D and S5E), establishing that this antibody was specific for the GrhO isoform. However, even with the O-isoform-specific antibody, we found that Grh levels were not significantly downregulated in the case of homozygotes for the single deletions (Fig-S5F-S5I). These observations collectively suggest that NB-specific Grh expression does not seem to rely solely on either of these two CREs (*Int-2BF1* or *Int-2C*).

CREs are often known to function redundantly to control the expression of a given gene. Therefore, upon deleting a particular CRE, the other CREs may show

increased activity [39, 40]. To test this, we checked if the deletion of the *Int-2BF1* or *Int-2C* led to increased activity of the other CREs (Fig 2G). This was done by checking the expression of *Ex1up-lacZ* and *Int-2C-lacZ* (inserted at Chr-3L-attp2-68A4) in the background of the deletion for *Int-2BF1 (ΔInt-2BF1* on Chr-2R*).* Similarly, we also checked the expression of *Ex1up-lacZ* and *Int-2BF1-lacZ* in the background of the deletion for *Int-2C (ΔInt-2C* on 2R*)*. However, contrary to our expectation, we observed that the activity of *Ex1up-lacZ* (Fig 2H-2I) and *Int-2C-lacZ* (Fig 2J-2K) was significantly downregulated in the case of *Int-2BF1* deletion homozygotes *(ΔInt-2BF1/ΔInt-2BF1)*. Similarly, the activity of *Ex1up-lacZ* (Fig 2L-2M) and *Int-2BF1-lacZ* (Fig 2N-2O) was also significantly downregulated in the case of *Int-2C* deletion homozygotes *(ΔInt-2C/ΔInt-2C)* (Fig 2P-2S), which suggests a possible physical interaction among these enhancers. Since *Int-2BF1* and *Int-2C* CREs are located close by in the second intron (approximately 3 Kb apart, Fig 2G), and the effect of *Int-2C* deletion on the expression of *Int-2BF1-lacZ* (on 3L) was most pronounced (Fig-2O'), we considered deleting these two CREs together.

**Double deletion of *Int-2BF1* and *Int-2C* reduces Grh expression in NBs.**

To test the collaborative functioning of *Int-2BF1* and *Int-2C,* we made a double deletion for the two CREs. The double deletion was referred to as *ΔInt-2BF1-ΔInt-2C'* (*grh$^{DD}$)* since the extent of *Int-2C* deletion was different in this case compared to the original *Int-2C* deletion (Table II). The double deletion was homozygous lethal as embryos, but the trans-heterozygotes of double deletion and *grh* deficiency (*grh$^{DD}$/grh$^{Df}$*) survived till the adult stage, indicating the existence of a third site modifier in the double deletion chromosome, which is a non-specific mutation outside *grh* locus considering that *grh$^{DD/Df}$* survived till adult stages. The

*grh*$^{DD}$/*grh*$^{Df}$ larval CNS showed a significant reduction in the expression of Grh from the NBs (Fig 3C vs 3C' and 3E' vs 3F'), with complete loss of Grh from a subset of NBs (yellow arrowheads, Fig 3E'' vs 3F'' and 3G), while the expression of Grh in the cells of wing discs was unaltered (Fig 3D vs 3D'). The Grh expression was also reduced in Type II NBs and their associated INPs (Fig S6G and S6H). The mild developmental delay observed in this case (*grh*$^{DD}$/*grh*$^{Df}$) was reminiscent of the delay seen in the case of trans-heterozygotes for *grh* deficiency and *grh*$^{370}$ (an allele of CNS specific O-isoform) (*grh*$^{370}$/*grh*$^{Df}$) [26]. Therefore, we also checked trans-heterozygotes of *grh*$^{DD}$ and *grh*$^{370}$ allele (*grh*$^{DD}$/*grh*$^{370}$) and observed a reduction in the levels of Grh from NBs of larval CNS (Fig S6A-S6D) without any change in the levels of Grh in the wing disc (Fig S6E), further corroborating the NB-specific role of the deleted enhancers. Thereafter, we checked if the reduction in the levels of *grh* (*grh*$^{DD}$/*grh*$^{Df}$) in CNS had any impact on abdominal NB apoptosis and thoracic NB proliferation in larval VNC [26]. We observed a partial block of apoptosis of abdominal and terminal NBs in larval VNC (Fig 3H and 3I) and proliferation defect in thoracic NBs homozygous mutant for *grh*$^{DD}$ (Fig 3J-3L).

These results established that *Int-2BF1* and *Int-2C* constitute one subset of CNS-specific CREs responsible for regulating the expression of *grh* in NBs. They also suggest that these two CREs are not required to regulate *grh* expression in larval wing discs, corroborating their NB-specific activity observed earlier. These results also imply that an enhancer may show activity in a specific tissue; however, the relevance of this activity (in cell physiology and tissue-specific gene expression) may need functional testing by deleting the enhancer.

**Epigenetic status of *grh* and its CREs in larval NBs, GMCs and neurons.**

Grh protein is known to be expressed in larval NBs and GMCs but not in the neurons; this is reiterated by the RNA-Seq results for NBs and neurons [41]. However, the epigenetic status of *grh* across these three cell types has not been elucidated so far. A previous study used Tada-Seq for five representative chromatin-binding proteins, namely **Brahma** (Brm: SWI/SNF ATPase chromatin remodeler associated with H3K27ac), **HP1** (an H3K9me3 reader, representative of HP1-associated heterochromatin), **Polycomb** (Pc an H3K27me3 reader, representing PcG chromatin), Histone **H1** (a linker histone, found in repressive black chromatin) and the core subunit of **RNA Polymerase II** (RNAP: indicating permissive and actively transcribed chromatin) and analysed their binding profile across the genome in three cells types of the CNS, namely NBs, GMC and neurons [7].

An underlying motivation to identify and functionally validate NB-specific enhancers (*Int-2BF1* and *Int-2C*) of *grh* was to check how the epigenetic status of a tissue-specific enhancer compared with that of the (*grh*) gene in a given cell type and to see how the two changes across the three cell types (NBs, GMCs and neurons). To this end, we analysed TaDa-seq data [7] and observed that the *grh* and the two deleted CREs show marks for RNAP and Brm in the larval NBs (Fig 4A and 4A'). In the case of GMCs, while the Brm marks were present on *grh* and CREs, RNAP showed very little occupancy on the two (Fig 4B and 4B' vs 4A and 4A'). In the case of the neurons, the *grh* and the two CREs did not show any occupancy by Brm and RNAP (Fig 4C and 4C'). For the repressive marks, we observed that in NBs and GMCs, significant Pc and HP1a marks were observed and H1 showed low occupancy on the *grh* locus and the two CREs (Fig 4A-4B). This suggests that *grh* is active in some and repressed in other lineages. This however changed in the case of neurons, where H1 and HP1a repressive marks were consistently observed on *grh*

and the two CREs (Fig 4C and 4C'), which is consistent with the fact that *grh* is not expressed in neurons in larval and pupal stages.

Importantly, RNA Pol II binding on *grh* indicated that it is actively transcribed in NBs but not in GMCs and neurons, suggesting that *grh* transcripts or proteins are most likely inherited by GMC from the NBs. To experimentally test this, we did a smFISH on larval CNS using *grh* probes. We observed that *grh* mRNA was primarily confined to NBs and not seen in GMC or neurons (Fig 5A). To further test this, we looked at the GMCs (marked by Ase) associated with the NBs (marked by Dpn), which show a complete loss of Grh expression in $grh^{DD}/grh^{Df}$ (pink arrowheads, Fig 5C''). Here, we observed that, like their mother NB, these GMCs did not express Grh (yellow arrowheads in Fig 5B'' vs 5C''). This would not be the case if GMCs were independently transcribing *grh,* reiterating that the GMCs inherit the Grh protein from the NBs.

These observations suggest that the epigenetic status of the *grh* and its tissue-specific CREs are broadly in sync with each other in vivo and synchronously change their states across different cell types of the developing CNS, which is in agreement with our result that deletion of these enhancers compromised Grh expression in NBs

## Discussion

Our study uses the CNS-specific expression of the *Drosophila grh* gene to make a case for deleting the enhancers to functionally validate their role in tissue-specific gene regulation. We find that *grh* regulation in NBs relies on multiple CREs, most likely with different enhancer combinations being important for regulating the expression in different subsets of NBs. Our results also suggest that multiple

enhancers may show activity in a specific cell type, but their role in gene regulation may be context-specific and become apparent only in a sensitized background of their deletion. Congruent to this, single deletions of two of CNS specific CREs did not impact the Grh expression in the CNS, and both the CREs had to be deleted together to show a significant reduction in Grh expression in the NBs and associated physiological phenotype in the CNS. This functionally corroborated the expression and utility of these enhancers in NBs and the absence of the phenotype for the double deletion on the Grh expression in non-neural tissue (wing discs).

The larval NB apoptosis mediated by the *RHG* family of apoptotic genes (*grim* and *reaper*) relied on a single enhancer [31]. This was expected owing to the limited developmental utility of these genes. Considering the diversity of its expression [13] and its role both as a pioneer TF and temporal TF (tTF), we expected Grh regulation to be more complex, relying on multiple CREs for its expression in different tissues (CNS and wing discs in our case). This was also underlined by a previous study in the vertebrates wherein one of the *grhl2* enhancers was deleted; however, no physiological phenotype was observed despite a 50% decrease in RNA transcripts [34]. This emphasized the robust and multi-modular transcriptional networks which may be regulating Grhl in the vertebrate system, suggesting that multiple enhancers may have to be deleted to see an impact on protein expression and physiology, which is what was found to be the case in case of *Drosophila grh.*

Our double deletion data can be interpreted in the light of the Source-Sink model used to explain epigenetic regulations of gene transcription [42], where genomic DNA operates as “Sink” and nucleosomes and epigenetic factors function as “Source.” The model suggests that different source proteins compete with each other for binding on the sink/DNA, thereby affecting genomic equilibrium and gene

regulation in a cell. An alternative way to think about it is the converse, where changing the sink availability could alter the overall free source levels. In NBs, if the enhancers were considered sinks, factors regulating *grh* transcription (activators and repressors) would be considered sources. Now, if one assumes that in the NBs, multiple enhancers are active, the free levels of repressive factor would normally be negligible, and the activating factors can bind to the *grh* gene and maintain the Grh protein expression at a certain level in these cells. Deletion of one enhancer does not affect this balance sufficiently, but the double-deletion increases the free repressor levels in cytoplasm beyond a threshold, thereby interfering with activating factors and impacting *grh* expression. This also explains an overall decrease in the levels of Grh in all the NBs of the CNS. The few cells where Grh expression is completely abrogated are the cells where these two deleted enhancers are critical for maintaining active gene expression.

We found *Ex1up* to be the only enhancer expressed in the wing disc; considering the enhancer redundancy for *grh* regulation in CNS, we expect that there might be other CREs outside the genomic region bracketed by the Type I insulator elements (selected by us for initial screening of enhancers) [38] which may regulate *grh* expression both in NB and wing discs. Grh is known to function both as a pioneer TF [19] [20] and tTF [21, 24, 25], but it is not clear whether these functions are associated with a specific isoform. With the generation of O isoform-specific Grh antibody, it may be possible to address isoform-specific roles of Grh [13]. However, assaying the expression of N isoform of Grh in a tissue will still be challenging.

Our analysis also suggests that existing TaDa-seq data [7] is a useful resource for mining the epigenetic status of genes/enhancers in the cells of CNS. By reanalysing this data, we find that *grh* shows RNAP, Brm and Pc marks in the NBs

and transitions into an RNAP negative and HP1a and Pc positive repressed state in GMCs and also shows additional repressive H1 marks in neurons. This broadly correlated with the epigenetic marks on the two enhancers we deleted (*Int-2BF1 and Int-2C*). Pc and HP1a marks on *grh* in NBs suggest that all the NB lineages may not express Grh simultaneously, corroborating our previous finding for NBs in the terminal region (in A8-A10 segments). These NBs show a temporal delay in initiating Grh expression compared to their thoracic and abdominal counterparts [31]. This analysis also suggested that *grh* is transcribed in NBs, and the protein is most likely inherited from NBs to GMCs. Most importantly, the analysis indicates that tissue-specific CREs are broadly in sync with the chromatin state of the *grh* gene in specific cell types of the CNS. However, how the epigenetic status of the gene changes in CNS when the tissue-specific enhancers are deleted needs to be tested experimentally. Considering the role of Grh as a tTF, it will be interesting to investigate the effect of the double deletion of CREs on the generation of cellular diversity in CNS.

## Materials and methods

### Fly stocks and fly husbandry.

The following fly lines were used in this study: *Canton-S* (BDSC-64349), *UAS-dcr2; inscGAL4-UASmCD8-GFP* [43], *Notch*$^{RNAi}$ (BDSC-28981), *PntGal4-UASmCD8-GFP* (Jurgen Knoblich, IMP, Vienna, Austria), *grh GAL4* (BDSC-64345). Egg collections were done for 4 hr, and flies were grown at 25ºC until the desired time points of dissection. The L1 and L2 stages were divided into three 8 hour intervals to define the early, mid, and late stages; for L3, this interval was 16 hours. The age was calculated as the hours after egg laying (AEL).

### Generation of transgenic flies

*Ex1up-lacZ*, *Int-1-lacZ*, *Int-2A-lacZ, Int-2BF1AB-3X-lacZ*, *Int-2C-lacZ*, *Int-3-lacZ*, *Int-7-lacZ*, *Int-8-lacZ, Int-9-lacZ*, *Int-11-lacZ, Int-14- lacZ* transgenic lines are generated using hs43-nuc-lacZ vector [44] modified for by site-specific insertion (referred to as *reporter-lacZ* here). All the constructs were inserted at attP2-68A4 on Chr-3L using phiC31-based integration system [45].

*Int-2BF1A-lacZ*, *Int-2BF1B-lacZ*, *Int-2BF1A'-lacZ*, *Int-2BF1*B'*-lacZ*, *Int-2BF1AB-lacZ*, *Int-2BF2-lacZ*, *Int-2BF3-lacZ* were generated using hs43-nuc-lacZ vector [44] by P-element-mediated transformation.

The enhancers were PCR amplified using region-specific primers and cloned into appropriate *reporter-lacZ* vectors.

### Immunohistochemistry and image acquisition

Brains of the desired larval stages were dissected and fixed in 4% paraformaldehyde in 1x PBS containing 0.3% TritonX-100 for 30 min at room temperature (RT) and followed by washing with 1X PBS containing 0.3% Triton X-100 for 30 minutes at RT.

Then the brains were immunostained with primary antibodies overnight at 4˚C. Embryos of stage 16th were stained as previously described [46]. The following primary antibodies were used: rabbit anti-Dpn (1:5,000; Bioklone, Chennai), rabbit anti-Grh (1: 2,000; Bioklone), chicken anti-β-gal (1: 2,000, ab9361, Abcam), Ase (CDFD animal house, 1:1000), Grh Exon 4+5(this study, CDFD animal house, 1:1000). Secondary antibodies conjugated to Alexa fluorophores from Molecular Probes were used: Alexa Fluor 405 (1:250), Alexa Fluor 488 (1:500), Alexa Fluor 555 (1:1,000), and Alexa Fluor 647 (1:500). The samples were mounted in 70% glycerol. Images were acquired with Zeiss LSM 900 confocal microscope and processed using ImageJ and Adobe Photoshop CS3. Scale bars are in µm and mentioned in the figure legends. White and pink arrowheads point NBs in all the figures; GMCs are indicated by yellow arrowheads. All the experiments were repeated at least 3 times, with controls and tests processed and imaged simultaneously in the same settings. All the images are representative of a minimum of 7 CNS specimens analysed.

**smFISH-IF protocol**

The smFISH was performed by following the protocol described in literature [47]. BioSearch probe designer was used to design the probes for *grh* gene against the coding sequence. 20nt probes were generated and checked for the off-targets. Generated probe (total 47) sequences were sent to Biosearch Technologies for synthesis with Fluorophore Quasar 570. In brief, larval CNS were dissected from 3rd instar larvae in 1xPBS and fixed in 4% paraformaldehyde in 1x PBS containing 0.3% TritonX-100(PBSTx) for 30 min at room temperature (RT) and followed by 3 quick washes with 1X PBS containing 0.3% Tween-20 (PBST). Brains were washed 3 times

for 15 minutes each at 25°C with PBST. Then, brains were incubated in wash buffer (10%v/v deionised formamide 1 in 2x saline sodium citrate (SSC)) solution for 5 mins at 37 °C. Then, brains were incubated in hybridization buffer (10% v/v deionized formamide, 10% v/v of 50% dextran sulphate solution (final dextran concentration = 5%) in 2x saline sodium citrate (SSC) solution) with the smFish probe concentration 0.5µm at 37° C for 8–15 hours with gentle rocking. For protein immunofluorescence, mouse anti-Grh (1:2000, Bioklone) was added in this step and incubated overnight. Thereafter, brains were rinsed 3 times in wash buffer. After this, brains were washed 3 times for 15 minutes each with wash buffer at 25° C. Next, brains were incubated with secondary antibody against Grh (Alexa Fluor 647) for 1 hour and 30 minutes at 25° C. Finally, brains were washed 3 times with wash buffer for 10 minutes each. The samples were mounted in 70% glycerol. Images were acquired with a Zeiss LSM 900 confocal microscope. Twelve specimens were analysed across three repetitions of the experiment, and a representative image is shown.

**CRISPR-Cas9 deletion of Grh enhancers**

The individual deletions of the *Int-2BF1* and *Int-2C* were performed using a double gRNA/Cas9-based strategy as described in [4]. The following guide RNA sequences were chosen:

Left guide for *Int-2BF1* deletion: GCATATGCCCCGCAGATCC

Right guide for *Int-2BF1* deletion: GGTAGTACTGTGAGAATTAC

Left guide for *Int-2C* deletion: GAGGAATATATGACATTAGT

Right guide for *Int-2C* deletion: GTGCAAAGGAACCCATCATGT

Both the left and Right guides for both the enhancers were cloned into a double gRNA vector where each of the guides is expressed under its own U6 promoter [4]. The constructs were then integrated into the attP40 landing site on the second chromosome. The two gRNA-containing males were then crossed to females of nos-cas9, and the resultant offspring containing both the gRNA and the cas9 were obtained. These were then crossed to second chromosome balancer flies, and 25 independent stocks were subsequently established. These stocks are homozygosed and flies from each stock were tested for the presence or absence of deletion by PCR. Two independent stocks containing the desired deletion were obtained, and PCR mapped the breakpoints. The following primer pairs were used to screen for the deletion:

Primers for Δ*Int-2BF1* screening

*Amplicon A*: *CTGTACTCTGCAAGTGGTCC* and *TCGCTCTAGGTACATACCCTG*

*Amplicon B*: *AACCATCACACTTTGTCTGTC* and *GTATTTGTACGAGCATATGC*

Primers for Δ*Int-2C* screening

*Amplicon A*: *CAATTGGGCACATCGAATGGA* and *TCTGGCCATTGAGCTTTCC*

*Amplicon B*: *CAGTAACGCTCGGAATTTGC* and *ATCCTTGCGCAAGTCTTCG*

For the generation of the double deletion of CREs (Δ*Int-2BF1,* Δ*Int-2C*), females from fly strain Δ*Int-2BF1/SM6 Cyo; nos-cas9/TM6B,Tb* was crossed with the *Int-2C* double gRNA containing males and similar steps were followed as mentioned for the generation of single deletions. 70 individual lines were established and screened for deletion by PCR, and only 1 line tested positive for deletion of both the enhancers.

Primers for double mutant (Δ*Int-2BF1,* Δ*Int-2C*) screening

*Int-2BF1 Amplicon*:

*AACCATCACACTTTGTCTGTC* and *GTATTTGTACGAGCATATGC*

*Int-2C Amplicon*:

*CAATTGGGCACATCGAATGGA* and *TCTGGCCATTGAGCTTTCC*

Activity interaction experiments shown in Fig 2 were done with the following genotypes:

*w*; *grh*Δ*Int-2BF1/grh*Δ*Int-2BF1; Ex1up-lacZ-68A4/+*

*w*; *grh*Δ*Int-2BF1/grh*Δ*Int-2BF1; Int-2C-lacZ-68A4/+*

*w*; *grh*Δ*Int-2C/grh*Δ*Int-2C; Ex1up-lacZ-68A4/+*

*w*; *grh*Δ*Int-2C/grh*Δ*Int-2C; Int-2BF1-lacZ-68A4/+*

**DamID-seq data processing**

To study the chromatin state of *grh* in NBs (neural stem cells), GMCs and neurons, bedgraphs were taken from previously published data [7] of different chromatin states (GEO GSE77860). Scaled averaged bedGraphs were downloaded as each dataset is divided by its standard deviation suitable for better comparison as described in the study.

All the five chromatin binding proteins were visualised in Integrated Genomic Viewer IGV for the binding on *grh* and its enhancers in the three datasets (NB, GMCs, neurons). The DamID tracks are generated using vector software pyGenomeTracks [48, 49].

## Figure Legends

**Fig 1. Expression analysis of *grh* enhancers.**

(A) Schematic of the genomic region of *grh* (exons are denoted by filled blue boxes, and blue lines denote the introns). All the genomics regions scanned by reporter lacZ assay are shown at the top of the reference sequence. Black lines denote the regions which showed no expression in larval NBs, and coloured boxes show regions that showed expression in late L3 stage NBs. The known *grh* enhancers like 4 Kb *grh-NB-lacZ* (covering 1.3 Kb *grh-NRE*) and 0.8 Kb *15B* are shown (in deep green, grey, and mud colours). The maroon box shows the position of 1.2 Kb *Int-2BF1*. (A') Schematic for Grh N, N', O and O' isoforms (adapted from Uv et al)[13]. (B-C) 1.2 Kb subfragment (*Int-2BF1*) (C) of 4 Kb enhancer *(Int-2B*) (B) recapitulates its activity in all the Grh expressing NBs. (D-E) In the Type I NBs, the *Int-2BF1-lacZ* is downregulated in response to Notch knockdown, but the levels of Grh protein are unaffected. (F-G) Novel CREs *Int-2C* and *Ex1up-lacZ* show activity in all the Grh-expressing NBs at the late L3 stage. (H-J) *Int-2BF1, Int-2C* and *Ex1up-lacZ* are also expressed in Type-II NBs (marked by *Pnt-GAL4>UAS-mCD8GFP*). NBs are marked with Deadpan (Dpn) in the late L3 stages. Notch knockdown in panels D-E is from the early embryonic stages. White arrowheads indicate Type II NBs. Scale bars are 50µm (for B-G) and 10µm (for D-E).

**Fig 2. *grh* enhancers *Int-2BF1* and *Int-2C* show activity action.**

(A-B) Shows the approximate positions of the guide RNAs and the size of the amplicons used to screen the deletions of *Int-2BF1* and *Int-2C*. Red and green lines show the extent of amplicons. (A'-B') Agarose gels confirming *Int-2BF1* (lanes 6 to

10 and 16-20) and *Int-2C* deletions (lanes 22 and 24) in the homozygotes larvae. Canton-S genomic is used as a wild-type control. (C-F) Shows that the Grh expression is unaffected in the NBs of heterozygous and homozygous deletions in the late L3 stage for *Int-2BF1* (C vs D) and *Int-2C* (E vs F). (C''' and E''') Show the quantitation graphs for Grh levels in heterozygous vs homozygous single deletions. (G) Schematic showing the approximate positions and sizes of *grh* enhancers *Ex1up* (yellow box)*, Int-2BF1* (brown box)*, and Int-2C* (green box) on Chr-2R and site of insertion of different *enhancer-lacZ* construct at attp2-68A4 on Chr-3L. (H-K) Homozygotes for *Int-2BF1* deletion (Δ*Int-2BF1*) show a significant reduction in the activity of *Ex1up-lacZ* (H vs I) and *Int-2C-lacZ* (J vs K) in late L3 stage NBs. (L-O) Homozygotes for *Int-2C* deletion (Δ*Int-2C*) show a significant reduction in the expression of *Ex1up-lacZ* (L vs M) and *Int-2BF1-lacZ* (N vs O) in late L3 stage NBs, (P-S) panels showing quantitation graphs for LacZ. White arrowheads indicate the NBs (shown in high magnification insets) marked by Deadpan (Dpn). Scale bars are 20 µm (for C-F), 30 µm (H-O) and 10 µm for the insets.

**Fig 3. Double deletion of *Int-2BF1* and *Int-2C* enhancers (*grh$^{DD}$*) compromises Grh expression in NBs but not in the epidermis.**

(A) Shows the approximate positions of the guide RNA sequences. Red and green lines show the extent of amplicons used for screening *Int-2BF1* and *Int-2C* deletions, respectively. *Int-2C* was deleted in the background of *Int-2BF1* deletion (Δ*Int-2BF1*). (B) Agarose gel confirming *Int-2BF1* (lanes 1 to 4) and *Int-2C* deletions (lanes 8 to 9) in the heterozygotes for the double deletion larvae (Δ*Int-2BF1,* Δ*Int-2C'/+* or *grh$^{DD}$*). Canton-S genomic is used as wild-type control; the extent of *Int-2C* deletion is different from the one shown in Fig 2 and is referred to as Δ*Int-2C'*. (C and E-F)

Compares the Grh expression in whole CNS (C vs C') and thoracic NBs of heterozygous *(grh$^{Df}$/+)* (E-E'') and heteroallelic combination of *grh* double deletion and deficiency (*grh$^{Df}$/grh$^{DD}$*) (F-F'') in the late L3 stage. The *grh$^{Df}$/grh$^{DD}$* shows a significant decrease in Grh expression in the NBs (white arrowheads), with some NBs showing a complete loss of Grh (yellow arrowheads), while the wing discs (D-D') do not show any change in Grh expression across the two genotypes. (G) Quantitative comparison of Grh levels in the larval Type I NBs in control and heteroallelic combination (*grh$^{Df}$/grh$^{DD}$*). (H) *grh$^{Df}$/grh$^{DD}$* shows a block of NB apoptosis in larval VNC. Terminal region (A8-A10) of the late L3 stage female VNC of *grh$^{Df}$/grh$^{DD}$* shows a block of NB apoptosis (H') compared to the heterozygous *(grh$^{DD}$/+)* control (H). (I) Shows the graphical comparison of the surviving NBs in A3-A10 segments of late L3 stage VNC. (J-L) MARCM clones for NBs with *grh$^{DD}$* (J) show a reduction in Grh levels (K) and decreased cell proliferation (L) at the late L3 stage. NBs marked with Deadpan (Dpn). Yellow arrowheads indicate NBs, which show loss of Grh expression; white arrowheads point to NBs, showing no change in Grh expression. Scale bars for C-D, G-G' are 30 µm, and E-F, H and J are 10µm, respectively.

**Fig 4. Epigenetic status of *grh* and its tissue-specific CREs are in sync in the NBs, GMC and neurons.**

(A-C') Occupancy profile of five chromatin marker proteins on *grh* gene (A-C) and its enhancers *Int-2BF1* and *Int-2C* (A'-C') in NB, GMCs and neurons, respectively. The five chromatin markers are RNA Pol II (orange), Brm (red), HP1a (green), Pc (blue) and H1 (grey). The binding profiles suggest that epigenetic status of CREs is in sync with *grh* in the NBs, GMC and neurons. Y-axis limits set from -5 to 5 for occupancy

comparison across the tracks. Coloured lines above the panels show the genomic extent of *grh* gene (from Chr- 2R: 17,801,132 to 17,842,820, pink), *Int-2BF1* (Chr-2R: 17,815,305 to 17,816,495, brown) and *Int-2C* (Chr-2R: 17,819,456 to 17,820,999, cyan) are indicated in different colours and bracketed by dashed lines. The coordinates indicated at the top are in kilobases.

**Fig 5. *grh* is transcribed in NBs but not in GMCs.**

(A) smFISH detects *grh* mRNA in NB but not in GMC associated with it, or in other surrounding cells. Grh antibody is used to mark NBs and GMCs. (B) Comparison of the Grh expression in GMCs associated with the thoracic NBs of heterozygous *($grh^{Df}/+$)* control larvae versus heteroallelic ($grh^{Df}/grh^{DD}$) larvae (C). The subset of NBs that showed a complete loss of Grh expression in the heteroallelic ($grh^{Df}/grh^{DD}$) larvae also showed a complete loss of Grh from the GMCs, suggesting that *grh* is expressed only in NBs and Grh protein is most likely inherited from NBs to GMCs. NBs and GMC are marked by white and yellow circumferences, respectively. White and pink arrowheads point to NBs, and yellow arrowheads show GMCs. Scale bar is 10 µm.

## Supplementary Figures

### Fig.S1. Sub-fragmentation of 4Kb *grh enhancer*

(A) Schematic for fragmentation of 4 Kb *grh* enhancer (*grh4/Int-2B*). (B-C) Subfragments of *Int-2BF1* (*Int-2BF1A* and *Int-2BF1B)* show activity in most Grh expressing NBs. (D) *Int-2BF1A'-lacZ* is expressed strongly in a subset of Grh-expressing NB of the central brain, and its expression in the VNC is highly reduced. (E) *Int-2BF1B'-lacZ* could be visualised only in a subset of Grh expressing NBs of the central brain and thoracic region of VNC. (F) The 150 bp overlap between *Int-2BF1A* and *Int-2BF1B* is expressed only in very few central brain cells and VNC cells. (G) The trimerised version of the 150 bp overlap *(Int-2BF1AB-3X-lacZ)* is expressed in the majority of the Grh-expressing NBs in the late L3 stage CNS. Scale bars are 50µm.

### Fig S2. Expression of *grh* CREs in larval CNS

(A-J) Shows the varying levels of activity of various *grh enhancer-lacZ* reporters (*Int-7, 8, 9, 11*, and *14*) in Type I NBs (A-E) and Type II NBs(F-J) of larval CNS. *Pnt-GAL4>UAS mCD8-GFP* is used to mark the Type II NBs in this case. *Int-7* showed some cells with very high and some with very low activity in NBs. *Int-8, 9, and 11* showed very weak activity in Type-I NBs and Type-II NBs. *Int-14* showed significant expression in both Type I and Type II NBs. (K-L) Shows the expression of *Int-10-GAL4>UAS-mCD8-GFP* (BDSC line 64345) in Type I and Type II NBs of late L3 stage larval CNS. *Int-10-GAL4* is strongly expressed in Type-II NBs and showed a very weak and limited expression in Type-I NBs. NBs are marked with either Dpn or Grh or Asense. Type II NBs in panels K-L are identified by $Dpn^{+}/Ase^{-}$ staining. White arrowheads indicate the NBs. Scale bars are 20µm.

**Fig S3. Expression of grh CREs in Wing Disc**

(A-C) Shows the expression of *Ex1up-lacZ* in wing discs of the late L3 larvae. Scale bars are 20µm.

**Fig S4. *Int-2BF1, Int-2C* and *Ex1up-lacZ* activity in A8-A10 NBs recapitulates the temporal increase of Grh seen from early L2 to early L3 stage.**

(A-I) Shows *Int-2BF1, Int-2C* and *Ex1up-lacZ* activity in A8-A10 NBs in early L2, late L2, and early L3 stages of development, NBs are marked with Dpn. White arrowheads indicate the expression of lacZ in terminal NBs. Scale bar is 20µm.

**Fig S5. The expression of CNS-specific GrhO isoform is unaltered in the single deletions for *Int-2BF1* and *Int-2C*.**

(A-A") GrhO isoform-specific antibody (Grh Exon4+5) (raised against 205 residues from Exon4+5) marks both NBs and GMCs in late L3 larval stage CNS of Canton S larvae. (B-C) Compares the staining of the antibodies raised against full-length Grh protein (GrhFL- detecting all the isoforms of Grh) and 205 residues from Exon4+5 (specific for GrhO isoform, Grh Exon4+5) in late L3 larval central brain and eye disc of Canton S larvae. GrhFL antibody shows expression in both CNS and eye discs, while GrhO (Grh Exon4+5) specific antibody detects Grh exclusively in CNS but not in the eye discs. (D-E) Compares the staining of Grh FL and GrhO specific (Grh Exon4+5) antibody in late L3 stage larval wing disc of Canton S larvae. (F-I) Shows that the expression of GrhO is unaltered in the heterozygotes and homozygotes for the single deletion of *Int-2BF1* (F-G) and *Int-2C* (H-I) in the thoracic NBs of late L3

stages CNS. NBs are marked by Deadpan (Dpn). Scale bars are 20 µm (A-C), 50 µm (D-E), 20 µm (D'-E'), 10 µm (F-I).

**Fig S6. Trans-heterozygotes for the GrhO specific allele (*grh$^{370}$*) and Double deletion of *Int-2BF1* and *Int-2C* enhancers (*grh$^{DD}$*) compromise Grh expression, specifically in NBs.**

(A-D) Compares the Grh staining in the late L3 stage CNS and thoracic NBs of heterozygous *(grh$^{370}$/+)* and heteroallelic combination (*grh$^{370}$/grh$^{DD}$*). The heteroallelic combination shows a dramatic decrease in Grh expression in the NBs, with some NBs showing a complete loss of Grh (similar to what is seen for *grh$^{Df}$/grh$^{DD}$*), while the wing discs (E-E') do not show any change in Grh expression across the two genotypes. (F) Quantitation of Grh intensity in the larval NBs of heterozygous *(grh$^{370}$/+)* and heteroallelic combination (*grh$^{370}$/grh$^{DD}$*). (G-I) Shows comparison of levels of Grh in Type-II NBs (G), associated INPs (H) and mitotic index in thoracic NBs of heterozygous (*grh$^{DD/+}$)* vs heteroallelic (*grh$^{Df/DD}$*) combinations of *grh.* NBs marked with Deadpan (Dpn). Scale bars for A-B, E and E' are 30 µm, and C-D are 10 µm.

## Acknowledgements

We thank R. Mann, J. Knoblich, S. Small, R. Rikhy, A. Ratnaparkhi, G. Ratnaparkhi, for various reagents and/or advice with experiments; D. Trivedi for her constant guidance and advice with the gRNA designs; BDSC, NIG-Fly, and DGRC -Japan stock centres for fly lines; DGRC -Japan for dual gRNA CRISPR-Cas9 constructs, CDFD animal facility, Bioklone Biotech Pvt. Ltd., Chennai and the Developmental Studies Hybridoma Bank at The University of Iowa for antibodies, Sophisticated Equipment Facility at CDFD for DNA sequencing and TFF at NCBS-CCAMP, Bangalore for transgenic flies. We thank Ch. Gangi Reddy for his advice and help with NGS data analysis, and C. S. Singh for his assistance in various phases of the project. This study was funded by; Department of Science and Technology, India (CRG/2021/003275); Department of Biotechnology, India (BT/PR41306/MED/122/259/2020; BT/PR45460/MED/12/952/2022); Wellcome Trust DBT India Alliance, India (Ref: 500171/Z/09/Z), CDFD core funds; and ICMR, India (award to R.S.) [ICMR Ref.No:3/1/3/JRF-2012/HRD-63 (40260)], CSIR, India (award to YR) [ File No:09/724(0132)/2018], UGC-JRF (award to JB) [UGC-No: F.16-6(DEC.2016)/2017(NET)].

## Author contribution

RJ conceptualised the study; RS, YR, JB, and PA did the experiments; RJ, RS, YR, and JB analysed the data; PA did the NGS data analysis; VK generated the double deletion. RJ wrote the manuscript.

## References


1. Horvath, P. and R. Barrangou, *CRISPR/Cas, the immune system of bacteria and archaea.* Science, 2010. **327**(5962): p. 167-70.
2. Mali, P., et al., *RNA-guided human genome engineering via Cas9.* Science, 2013. **339**(6121): p. 823-6.
3. Jinek, M., et al., *RNA-programmed genome editing in human cells.* Elife, 2013. **2**: p. e00471.
4. Kondo, S. and R. Ueda, *Highly improved gene targeting by germline-specific Cas9 expression in Drosophila.* Genetics, 2013. **195**(3): p. 715-21.
5. Gratz, S.J., et al., *CRISPR-Cas9 Genome Editing in Drosophila.* Curr Protoc Mol Biol, 2015. **111**: p. 31 2 1-31 2 20.
6. Southall, T.D., et al., *Cell-type-specific profiling of gene expression and chromatin binding without cell isolation: assaying RNA Pol II occupancy in neural stem cells.* Dev Cell, 2013. **26**(1): p. 101-12.
7. Marshall, O.J. and A.H. Brand, *Chromatin state changes during neural development revealed by in vivo cell-type specific profiling.* Nat Commun, 2017. **8**(1): p. 2271.
8. Bray, S.J., et al., *Embryonic expression pattern of a family of Drosophila proteins that interact with a central nervous system regulatory element.* Genes Dev, 1989. **3**(8): p. 1130-45.
9. Kudryavtseva, E.I., et al., *Identification and characterization of Grainyhead-like epithelial transactivator (GET-1), a novel mammalian Grainyhead-like factor.* Dev Dyn, 2003. **226**(4): p. 604-17.
10. Ting, S.B., et al., *A homolog of Drosophila grainy head is essential for epidermal integrity in mice.* Science, 2005. **308**(5720): p. 411-3.
11. Wilanowski, T., et al., *A highly conserved novel family of mammalian developmental transcription factors related to Drosophila grainyhead.* Mech Dev, 2002. **114**(1-2): p. 37-50.
12. Prokop, A., et al., *Homeotic regulation of segment-specific differences in neuroblast numbers and proliferation in the Drosophila central nervous system.* Mech Dev, 1998. **74**(1-2): p. 99-110.
13. Uv, A.E., E.J. Harrison, and S.J. Bray, *Tissue-specific splicing and functions of the Drosophila transcription factor Grainyhead.* Mol Cell Biol, 1997. **17**(11): p. 6727-35.
14. Uv, A.E., C.R. Thompson, and S.J. Bray, *The Drosophila tissue-specific factor Grainyhead contains novel DNA-binding and dimerization domains which are conserved in the human protein CP2.* Mol Cell Biol, 1994. **14**(6): p. 4020-31.
15. Chen, W., et al., *Grainyhead-like 2 regulates epithelial plasticity and stemness in oral cancer cells.* Carcinogenesis, 2016. **37**(5): p. 500-10.
16. Mlacki, M., et al., *Loss of Grainy head-like 1 is associated with disruption of the epidermal barrier and squamous cell carcinoma of the skin.* PLoS One, 2014. **9**(2): p. e89247.
17. Xu, H., et al., *Clinical implications of GRHL3 protein expression in breast cancer.* Tumour Biol, 2014. **35**(3): p. 1827-31.
18. Nevil, M., et al., *Stable Binding of the Conserved Transcription Factor Grainy Head to its Target Genes Throughout Drosophila melanogaster Development.* Genetics, 2017. **205**(2): p. 605-620.

19. Jacobs, J., et al., *The transcription factor Grainy head primes epithelial enhancers for spatiotemporal activation by displacing nucleosomes.* Nat Genet, 2018. **50**(7): p. 1011-1020.
20. Nevil, M., et al., *Establishment of chromatin accessibility by the conserved transcription factor Grainy head is developmentally regulated.* Development, 2020. **147**(5).
21. Brody, T. and W.F. Odenwald, *Programmed transformations in neuroblast gene expression during Drosophila CNS lineage development.* Dev Biol, 2000. **226**(1): p. 34-44.
22. Allan, D.W. and S. Thor, *Transcriptional selectors, masters, and combinatorial codes: regulatory principles of neural subtype specification.* Wiley Interdiscip Rev Dev Biol, 2015. **4**(5): p. 505-28.
23. Miyares, R.L. and T. Lee, *Temporal control of Drosophila central nervous system development.* Curr Opin Neurobiol, 2019. **56**: p. 24-32.
24. Doe, C.Q., *Temporal Patterning in the Drosophila CNS.* Annu Rev Cell Dev Biol, 2017. **33**: p. 219-240.
25. Bayraktar, O.A. and C.Q. Doe, *Combinatorial temporal patterning in progenitors expands neural diversity.* Nature, 2013. **498**(7455): p. 449-55.
26. Cenci, C. and A.P. Gould, *Drosophila Grainyhead specifies late programmes of neural proliferation by regulating the mitotic activity and Hox-dependent apoptosis of neuroblasts.* Development, 2005. **132**(17): p. 3835-45.
27. Almeida, M.S. and S.J. Bray, *Regulation of post-embryonic neuroblasts by Drosophila Grainyhead.* Mech Dev, 2005. **122**(12): p. 1282-93.
28. Bello, B.C., F. Hirth, and A.P. Gould, *A pulse of the Drosophila Hox protein Abdominal-A schedules the end of neural proliferation via neuroblast apoptosis.* Neuron, 2003. **37**(2): p. 209-19.
29. Khandelwal, R., et al., *Combinatorial action of Grainyhead, Extradenticle and Notch in regulating Hox mediated apoptosis in Drosophila larval CNS.* PLoS Genet, 2017. **13**(10): p. e1007043.
30. Ghosh, N., et al., *Hox gene Abdominal-B uses Doublesex(F) as a cofactor to promote neuroblast apoptosis in Drosophila central nervous system.* Development, 2019.
31. Bakshi, A., et al., *Sequential activation of Notch and Grainyhead gives apoptotic competence to Abdominal-B expressing larval neuroblasts in Drosophila Central nervous system.* PLoS Genet, 2020. **16**(8): p. e1008976.
32. Sipani, R. and R. Joshi, *Hox genes collaborate with helix-loop-helix factor Grainyhead to promote neuroblast apoptosis along the anterior-posterior axis of the Drosophila larval central nervous system.* Genetics, 2022. **222**(1).
33. Chai, P.C., et al., *Hedgehog signaling acts with the temporal cascade to promote neuroblast cell cycle exit.* PLoS Biol, 2013. **11**(2): p. e1001494.
34. de Vries, M., et al., *Interrogating the Grainyhead-like 2 (Grhl2) genomic locus identifies an enhancer element that regulates palatogenesis in mouse.* Dev Biol, 2020. **459**(2): p. 194-203.
35. An, H., et al., *Pipsqueak family genes dan/danr antagonize nuclear Pros to prevent neural stem cell aging in Drosophila larval brains.* Front Mol Neurosci, 2023. **16**: p. 1160222.
36. Zacharioudaki, E., et al., *Genes implicated in stem cell identity and temporal programme are directly targeted by Notch in neuroblast tumours.* Development, 2016. **143**(2): p. 219-31.

37. Kuzin, A., et al., *Structure and cis-regulatory analysis of a Drosophila grainyhead neuroblast enhancer.* Genesis, 2018. **56**(3): p. e23094.
38. Negre, N., et al., *A comprehensive map of insulator elements for the Drosophila genome.* PLoS Genet, 2010. **6**(1): p. e1000814.
39. Carleton, J.B., K.C. Berrett, and J. Gertz, *Multiplex Enhancer Interference Reveals Collaborative Control of Gene Regulation by Estrogen Receptor alpha-Bound Enhancers.* Cell Syst, 2017. **5**(4): p. 333-344 e5.
40. Osterwalder, M., et al., *Enhancer redundancy provides phenotypic robustness in mammalian development.* Nature, 2018. **554**(7691): p. 239-243.
41. Berger, C., et al., *FACS purification and transcriptome analysis of drosophila neural stem cells reveals a role for Klumpfuss in self-renewal.* Cell Rep, 2012. **2**(2): p. 407-18.
42. Murphy, P.J. and F. Berger, *The chromatin source-sink hypothesis: a shared mode of chromatin-mediated regulations.* Development, 2023. **150**(21).
43. Neumuller, R.A., et al., *Genome-wide analysis of self-renewal in Drosophila neural stem cells by transgenic RNAi.* Cell Stem Cell, 2011. **8**(5): p. 580-93.
44. Estella, C., D.J. McKay, and R.S. Mann, *Molecular integration of wingless, decapentaplegic, and autoregulatory inputs into Distalless during Drosophila leg development.* Dev Cell, 2008. **14**(1): p. 86-96.
45. Bischof, J., et al., *An optimized transgenesis system for Drosophila using germ-line-specific phiC31 integrases.* Proc Natl Acad Sci U S A, 2007. **104**(9): p. 3312-7.
46. Noro, B., et al., *Distinct functions of homeodomain-containing and homeodomain-less isoforms encoded by homothorax.* Genes Dev, 2006. **20**(12): p. 1636-50.
47. Yang, L., et al., *Single molecule fluorescence in situ hybridisation for quantitating post-transcriptional regulation in Drosophila brains.* Methods, 2017. **126**: p. 166-176.
48. Ramirez, F., et al., *High-resolution TADs reveal DNA sequences underlying genome organization in flies.* Nat Commun, 2018. **9**(1): p. 189.
49. Lopez-Delisle, L., et al., *pyGenomeTracks: reproducible plots for multivariate genomic datasets.* Bioinformatics, 2021. **37**(3): p. 422-423.

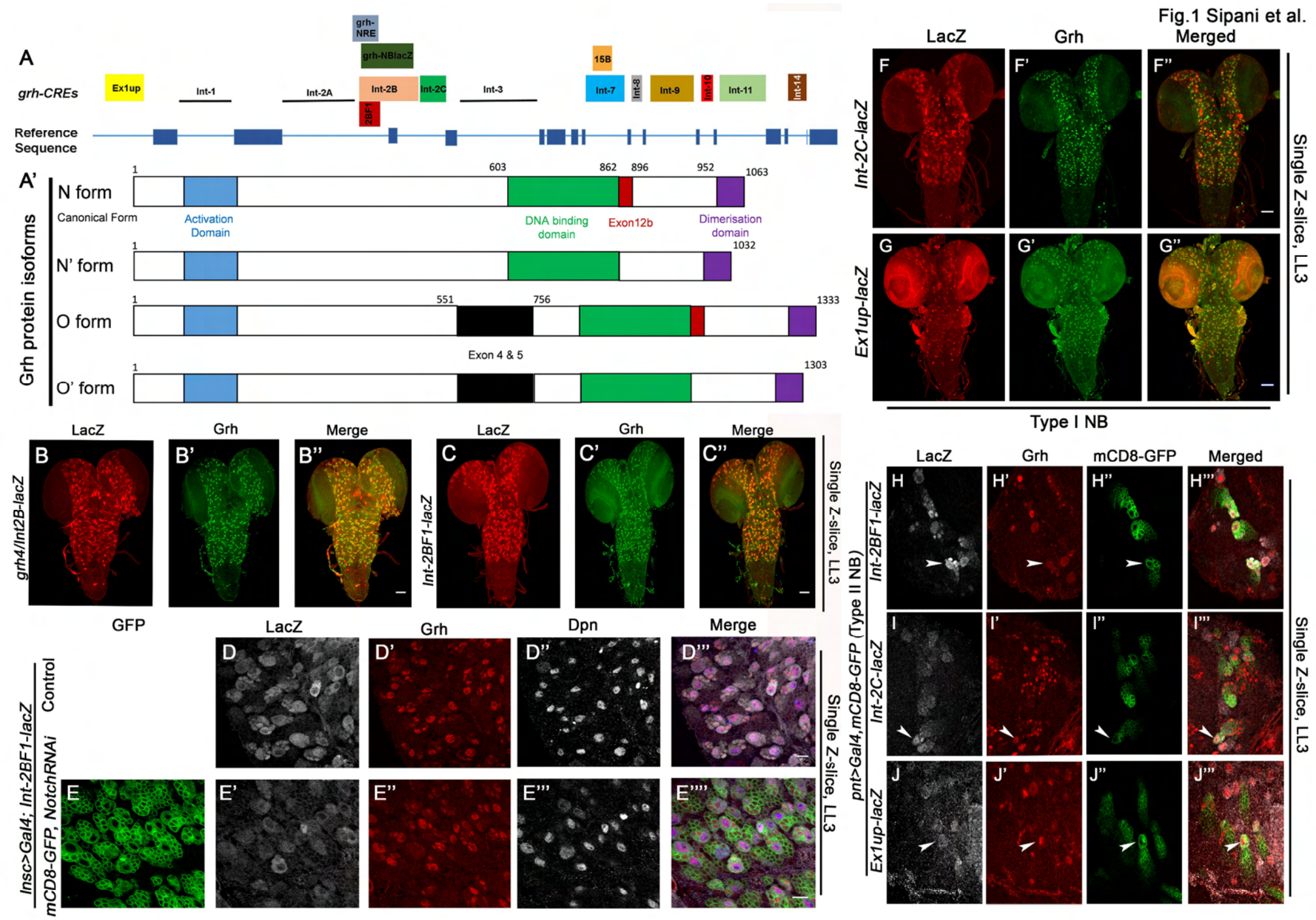
Fig.1 Sipani et al.
A
grh-CREs
Ex1up
Int-1
Int-2A
grh-NRE
grh-NBlacZ
Int-2B
Int-2C
2BF1
Int-3
15B
Int-7
Int-8
Int-9
Int-10
Int-11
Int-14
Reference Sequence
A'
Grh protein isoforms
N form
Canonical Form
Activation Domain
DNA binding domain
Exon12b
Dimerisation domain
N' form
O form
Exon 4 & 5
O' form
LacZ
Grh
Merge
Int-2C-lacZ
Ex1up-lacZ
Single Z-slice, LL3
Type I NB
grh4/Int2B-lacZ
Int-2BF1-lacZ
GFP
Dpn
Insc>Gal4; Int-2BF1-lacZ
mCD8-GFP, NotchRNAi
Control
mCD8-GFP
pnt>Gal4,mCD8-GFP (Type II NB)

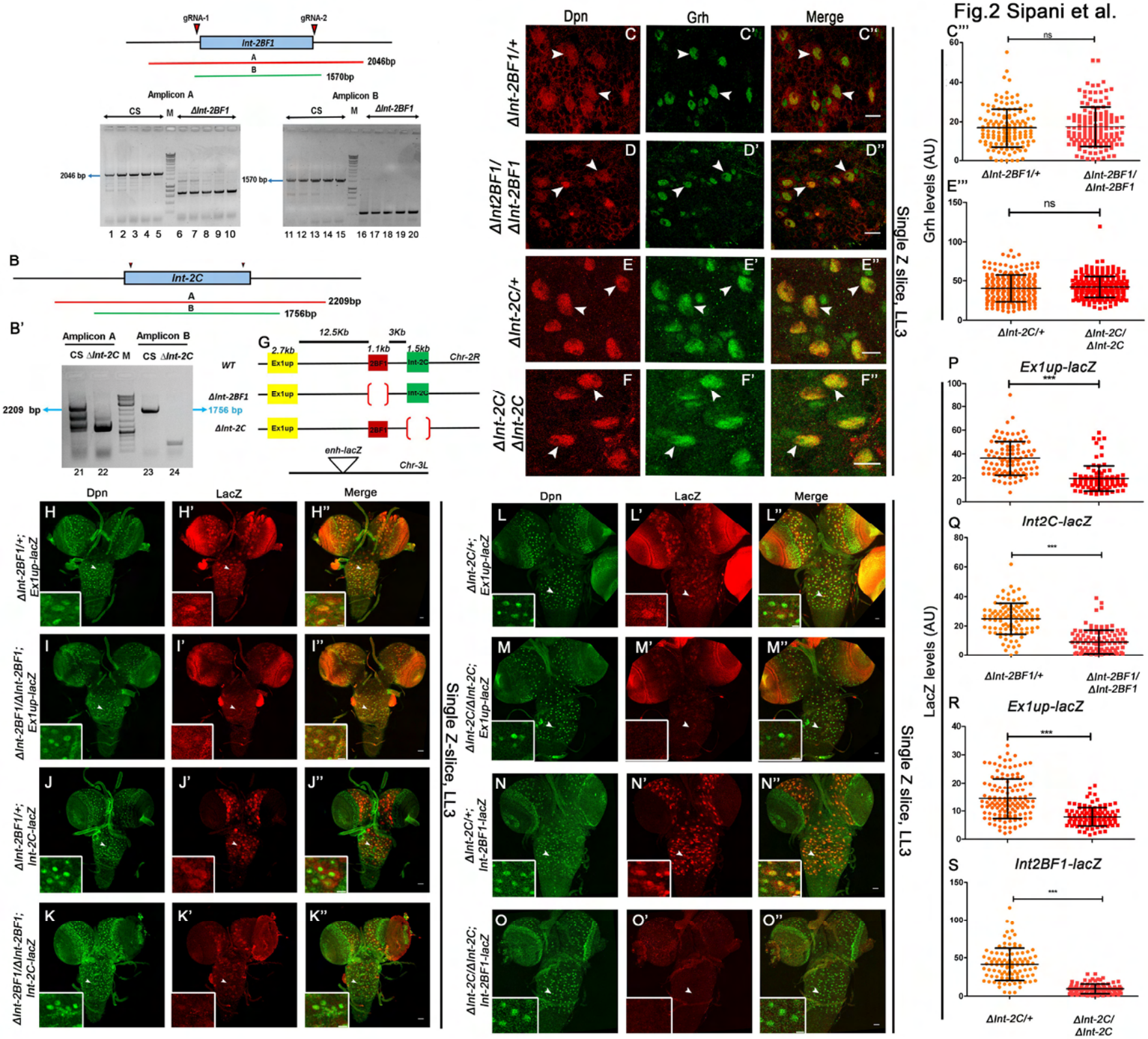

Fig.2 Sipani et al.
gRNA-1
gRNA-2
Int-2BF1
A
2046bp
B
1570bp
Amplicon A
Amplicon B
CS
M
ΔInt-2BF1
2046 bp
1570 bp
1 2 3 4 5 6 7 8 9 10
11 12 13 14 15 16 17 18 19 20
B
Int-2C
2209bp
1756bp
B'
Amplicon A
Amplicon B
CS ΔInt-2C M
CS ΔInt-2C
2209 bp
1756 bp
21 22 23 24
G
12.5Kb
3Kb
2.7kb
1.1kb
1.5kb
WT
ΔInt-2BF1
ΔInt-2C
Ex1up
2BF1
Int-2C
Chr-2R
enh-lacZ
Chr-3L
Dpn
Grh
Merge
ΔInt-2BF1/+
ΔInt2BF1/ ΔInt-2BF1
ΔInt-2C/+
ΔInt-2C/ ΔInt-2C
Single Z slice, LL3
Grh levels (AU)
ns
LacZ levels (AU)
Ex1up-lacZ
Int2C-lacZ
Int2BF1-lacZ
***
LacZ
ΔInt-2BF1/+; Ex1up-lacZ
ΔInt-2BF1/ΔInt-2BF1; Ex1up-lacZ
ΔInt-2BF1/+; Int-2C-lacZ
ΔInt-2BF1/ΔInt-2BF1; Int-2C-lacZ
ΔInt-2C/+; Ex1up-lacZ
ΔInt-2C/ΔInt-2C; Ex1up-lacZ
ΔInt-2C/+; Int-2BF1-lacZ
ΔInt-2C/ΔInt-2C; Int-2BF1-lacZ
Single Z-slice, LL3

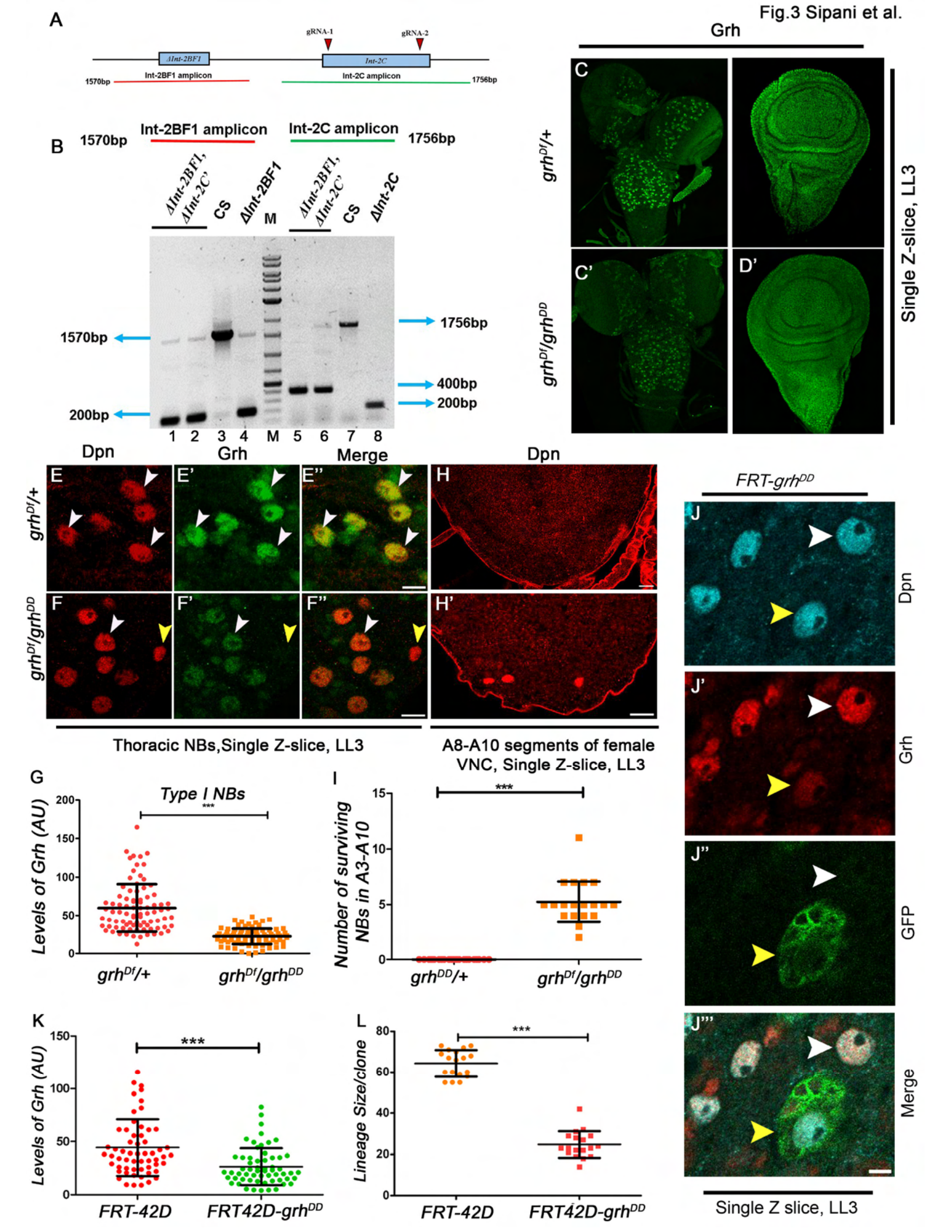
A
gRNA-1
gRNA-2
ΔInt-2BF1
Int-2C
Int-2BF1 amplicon
Int-2C amplicon
1570bp
1756bp
B
1570bp
Int-2BF1 amplicon
Int-2C amplicon
1756bp
ΔInt-2BF1, ΔInt-2C'
CS
ΔInt-2BF1
M
ΔInt-2BF1, ΔInt-2C'
CS
ΔInt-2C
1570bp
200bp
1756bp
400bp
200bp
1 2 3 4 M 5 6 7 8
Grh
C
C'
D'
grhDf/+
grhDf/grhDD
Single Z-slice, LL3
Dpn
Grh
Merge
Dpn
E
E'
E''
H
F
F'
F''
H'
grhDf/+
grhDf/grhDD
Thoracic NBs,Single Z-slice, LL3
A8-A10 segments of female VNC, Single Z-slice, LL3
FRT-grhDD
J
J'
J''
J'''
Dpn
Grh
GFP
Merge
Single Z slice, LL3
G
Type I NBs
Levels of Grh (AU)
200
150
100
50
0
***
grhDf/+
grhDf/grhDD
I
Number of surviving NBs in A3-A10
15
10
5
0
***
grhDD/+
grhDf/grhDD
K
Levels of Grh (AU)
150
100
50
0
***
FRT-42D
FRT42D-grhDD
L
Lineage Size/clone
80
60
40
20
0
***
FRT-42D
FRT42D-grhDD

Fig4 Sipani et al.

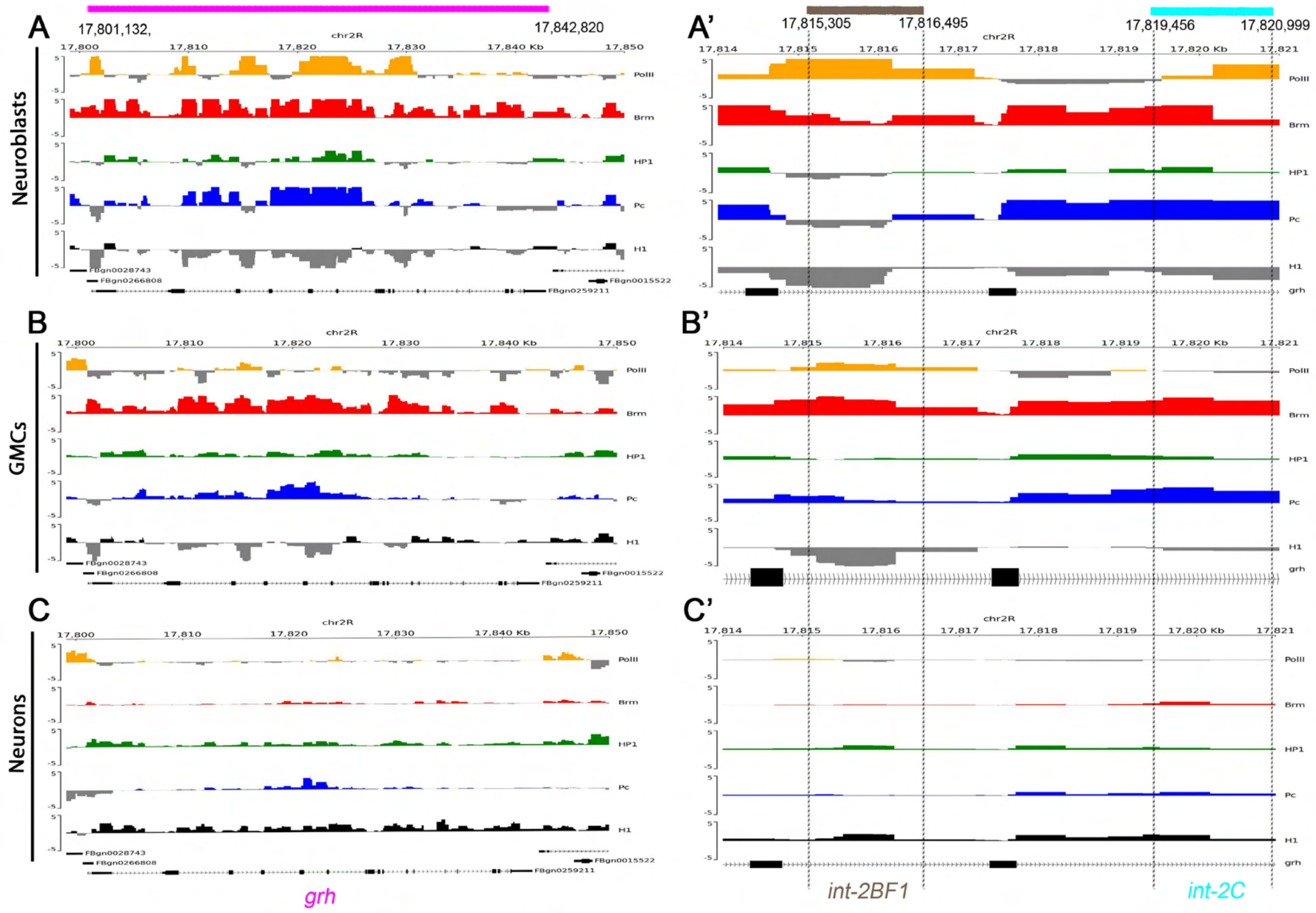
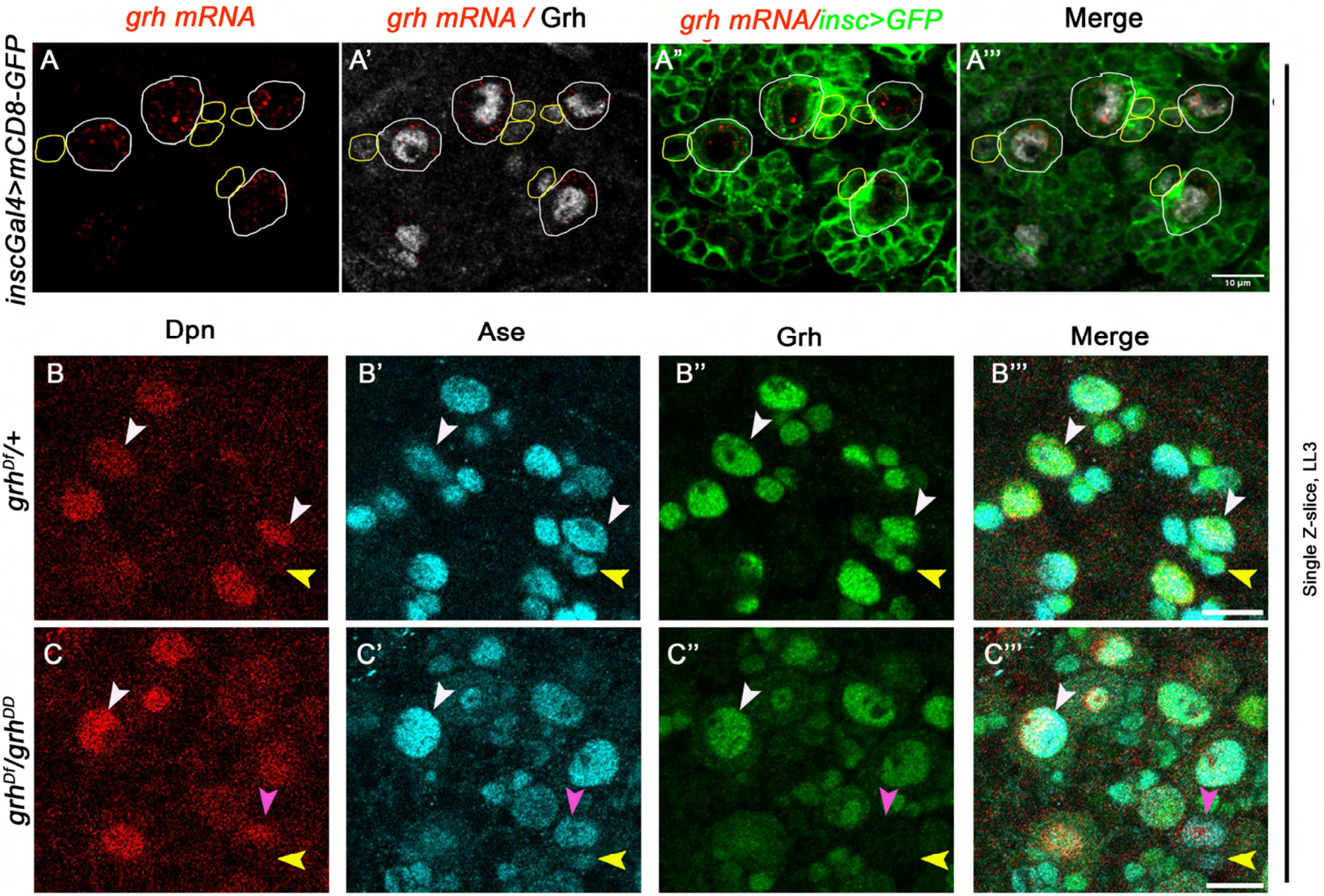
Fig 5 Sipani et al.